# Limited and strain-specific transcriptional and growth responses to acquisition of a multidrug resistance plasmid in genetically diverse *Escherichia coli* lineages

Steven Dunn*[1], Laura Carrilero*[2], Michael Brockhurst[2], Alan McNally[1]

*Joint first authors contributed equally

[1]Institute of Microbiology and Infection, College of Medical and Dental Science, University of Birmingham, Birmingham B15 2TT

[2]Division of Evolution and Genomic Sciences, School of Biological Sciences, University of Manchester, Manchester M13 9PT

Running title: Transcriptional response to MDR plasmids in *E. coli*

**Abstract**

Multi-drug resistant (MDR) *Escherichia coli* are a major global threat to human health, wherein multi-drug resistance is primarily spread by MDR plasmid acquisition. MDR plasmids are not widely distributed across the entire *E. coli* species, but instead are concentrated in a small number of clones. Here, we test if diverse *E. coli* strains vary in their ability to acquire and maintain MDR plasmids, and if this relates to their transcriptional response following plasmid acquisition. We used strains from across the diversity of *E. coli*, including the common MDR lineage ST131, and the IncF plasmid, pLL35, encoding multiple antibiotic resistance genes. Strains varied in their ability to acquire pLL35 by conjugation, but all were able to stably maintain the plasmid. The effects of pLL35 acquisition on cefotaxime resistance and growth also varied among strains, with growth responses ranging from a small decrease to a small increase in growth of the plasmid-carrier relative to the parental strain. Transcriptional responses to pLL35 acquisition were limited in scale and highly strain specific. We observed significant transcriptional responses at the operon or regulon level, possibly due to stress responses or interactions with resident MGEs. Subtle transcriptional responses consistent across all strains were observed affecting functions, such as anaerobic metabolism, previously shown to be under negative frequency dependent selection in MDR *E. coli*. Overall, there was no correlation between the magnitude of the transcriptional and growth responses across strains. Together these data suggest that fitness costs arising from transcriptional disruption are unlikely to act as a barrier to dissemination of this MDR plasmid in *E. coli*.

40 **Importance**

41 Plasmids play a key role in bacterial evolution by transferring niche adaptive functions
42 between lineages, including driving the spread of antibiotic resistance genes. Fitness
43 costs of plasmid acquisition arising from the disruption of cellular processes could limit
44 the spread of multidrug resistance plasmids. However, the impacts of plasmid
45 acquisition are typically measured in lab-adapted strains rather than in more
46 ecologically relevant natural isolates. Using a clinical multidrug resistance plasmid and
47 a diverse collection of *E. coli* strains isolated from clinical infections and natural
48 environments, we show that plasmid acquisition had only limited and highly strain-
49 specific effects on bacterial growth and transcription. These findings suggest that
50 fitness costs arising from transcriptional disruption are unlikely to act as a barrier to
51 transmission of this plasmid in natural populations of *E. coli*.

52

53 **Introduction**

54 Multi-drug resistant (MDR) *Escherichia coli* present a global public health risk and are
55 listed by the World Health Organisation as a priority pathogen. The incidence of MDR
56 *E. coli* as aetiological agents of human disease has steadily increased since the turn
57 of the century (Mathers et al., 2015). Initially this was due to the emergence of *E. coli*
58 clones carrying plasmids containing extended spectrum beta-lactamase (ESBL)
59 genes conferring resistance to third generation cephalosporins (Mathers et al., 2015).
60 This emergence mirrored the rise in the incidence of *E. coli* as the causative agent of
61 bloodstream infections world-wide, primarily due to the rapid global dissemination of
62 MDR clones (Banerjee & Johnson, 2014; Mathers et al., 2015). This was followed by
63 the emergence of clones carrying plasmids encoding carbapenemase enzyme genes,
64 conferring strains resistance to all antimicrobial classes with the exception of colistin
65 (Peirano et al., 2011; Wu et al., 2019).

66

67 The emergence of MDR *E. coli* has not occurred evenly across this species. Rather
68 MDR plasmid carriage is concentrated in a number of clones associated with extra-
69 intestinal infections, whilst it is rarely seen in clones causing intestinal infectious
70 disease or in exclusively commensal lineages (Dunn et al., 2019). ESBL plasmid
71 carriage is most commonly seen in low-diversity clones of lineages such as ST131,
72 ST648, and ST410 (Dunn et al., 2019), with ST131 representing the most common
73 cause of MDR *E. coli* bloodstream and urine infections in the developed world
74 (Banerjee & Johnson, 2014). Carriage of carbapenemase encoding plasmids is also
75 concentrated in low-diversity clones of lineages such as ST167 and ST410, belonging
76 to the Phylogroup A clade of *E. coli* which are generally devoid of most common *E.*
77 *coli* virulence factors (Feng et al., 2019; Wu et al., 2019; Zong et al., 2018).

78

79 Comparison of the genomes of MDR plasmid carrying clones with the lineages that
80 those clones emerged from shows striking similarity in key steps in their evolution. All
81 show rapid clonal expansion of MDR plasmid carrying strains which become globally
82 distributed in a matter of years (Feng et al., 2019; Petty et al., 2014; Zong et al., 2018).
83 The MDR clones also carry clone specific alleles of key genes encoding traits involved
84 in human colonisation, such as adhesins and iron acquisition (Feng et al., 2019;
85 McNally et al., 2019; Zong et al., 2018). Comprehensive analysis of ST131 MDR clade
86 C showed it differed from the drug susceptible clade A and B of the lineage in a number
87 of unique alleles of genes involved in colonisation as well as anaerobic metabolism
88 genes (McNally et al., 2019). MDR clones also contain unique intergenic-sequence
89 alleles, which correlate with plasmids carried by strains (McNally et al., 2016)(Feng et
90 al., 2019; Zong et al., 2018).

91

92 As well as the biosynthetic burden associated with replicating, transcribing and
93 translating the new genetic material, plasmid acquisition often disrupts cellular
94 homeostasis. For example, large-scale changes to regulation of chromosomal genes
95 have been observed following plasmid acquisition in a range of bacterial hosts
96 (Harrison et al., 2015; Millan et al., 2015; San Millan et al., 2018), which can be
97 negated by compensatory mutations to regulators. The shared genetic traits of MDR
98 clones of *E. coli* including regulatory sequences together with the uneven distribution
99 of MDR plasmids, suggests that some lineages of *E. coli* may be better preadapted to
100 the acquisition and stable integration of MDR plasmids than others, potentially
101 suffering less cellular disruption (Dunn et al., 2019; McNally et al., 2016). However,

102 data comparing the transcriptional and phenotypic responses of diverse *E. coli* strains
103 to MDR plasmid acquisition are lacking.
104
105 We tested the transcriptional response to acquisition of pLL35, an ESBL plasmid
106 encoding CTX-M-15 and TEM-112, in eight genetically diverse *E. coli* strains, including
107 environmental *E. coli* isolates from lineages in which MDR plasmids have never been
108 reported, and strains from clade A, B and C of *E. coli* ST131, wherein clade C is most
109 frequently associated with MDR plasmid acquisition. Strains varied in the rate of pLL35
110 acquisition by conjugation from *K. pneumoniae* and the degree of cefotaxime
111 resistance conferred by the plasmid but not in stability of the plasmid once acquired.
112 pLL35 carriers showed variations in growth relative to plasmid free cells ranging from
113 impaired to enhanced relative growth of plasmid carriers. Plasmid transcription did not
114 vary significantly among host strains, but we observed strain specific differences in
115 chromosomal gene expression caused by plasmid acquisition. We observed no
116 correlation between the degree of transcriptional disruption caused by plasmid
117 acquisition and the relative growth of pLL35 carriers.
118

119 **Methods and materials**

120 **Bacterial strains and plasmids**

121 A total of 8 *E. coli* strains were selected for use in this study, representing sequence
122 types 131 (clades A, B, and C), 394, and 1122 (Table S1). All strains were screened
123 to ensure that they did not contain any existing MDR plasmids. This study used
124 plasmid donor strain LL35 (a *Klebsiella pneumoniae* isolate belonging to ST-45) which
125 contains pLL35, a 106 kb incFII(K)-9 plasmid with a complete conjugative transfer
126 machinery, and a complex antibiotic resistance region (Figure S1). The resistance

127 region in pLL35 is comprised of multiple translocatable genetic elements. It contains
128 several complete antibiotic resistance genes, conferring resistance to cephalosporins
129 and beta-lactams (*blaCTX-M-15*, *blaTEM-112*), aminoglycosides (*aacA4, aacC2,*
130 *aadA1*) and quinolones (*qnrS1*). This region also contains OXA-9, however this gene
131 is truncated due to a premature stop codon. The antibiotic resistance region is
132 potentially mobilizable, due to an ISEcp1 insertion sequence. pLL35 also encodes two
133 separate toxin/antitoxin systems (*higAB*, *ccdAB*).
134
135 **Plasmid conjugation**
136 Twelve independent conjugation assays were performed for each strain following an
137 end-point method (Simonsen et al., 1990). A single colony from overnight growth on
138 nutrient agar was inoculated into 5 ml of nutrient broth (Oxoid, UK). This was incubated
139 at 37˚C for 2 hours with shaking (180 rpm). Cultures were mixed at a ratio of 1:3 donor
140 to recipient and 50 µl were used to inoculate 6 ml of BHI. Six replicates were incubated
141 as static cultures at 37˚C for 24 hours, and six replicates were incubated as shaken
142 cultures at 37˚C for 24 hours at 180 rpm. Conjugation rate data were $\log_{10}$ transformed
143 for statistical analysis.
144
145 The conjugation mix was plated onto UTI Chromagar (Sigma Aldrich, UK)
146 supplemented with 4 µg/ml of cefotaxime and incubated at 37˚C overnight. Colonies
147 that produced a phenotype indicative of *E. coli* were further subcultured onto UTI
148 Chromagar with 4 µg/ml of cefotaxime in order to check the resistance profile, and to
149 ensure there was sufficient pure growth to store for subsequent use. One of these
150 replicates was used to quantify differential gene expression and is subsequently
151 referred to as the transconjugant. Whole genome sequencing (WGS) data was also

152 generated for three additional replicates from the conjugation assays, which are
153 referred to as the transconjugant replicates.
154
155 In the generation of conjugated strains, bacteria were sub-cultured a total of 5 times.
156 In order to account for any basal adaptation to the lab conditions, and to control for
157 any variation generated by variables extraneous to the plasmid conjugation, the
158 parental recipient strains were also run through the conjugation protocol with a plasmid
159 free *Klebsiella* strain Ecl8 (Buckner et al., 2018). These triplicate samples were also
160 sequenced and are referred to as the control replicates.
161
162 **Genome sequencing**
163 Whole genome sequencing was performed on the ancestral, transconjugant, control
164 replicates and transconjugant replicate strains. The ancestral and transconjugant lines
165 were sequenced by both Illumina and Oxford Nanopore based technologies. Illumina
166 sequencing was provided by MicrobesNG (http://www.microbesng.com). Illumina
167 genome sequence reads were assessed for quality using FastQC (V 0.11.9), and
168 subsequently trimmed using Trimmomatic (V 0.3)14 with a sliding window quality of
169 Q15 and length of 20 base pairs. Kraken (V 2) was used to confirm species ID and
170 check for potential contaminants.
171
172 Long read sequencing was performed on DNA extracted using a phenol/chloroform
173 method (Sambrook & Russell, 2006). DNA was quantified using the Qubit 4.0 and a
174 broad range dsDNA kit (ThermoFisher, UK). Libraries were prepared using the SQK-
175 LSK109 sequencing kit, and EXP-NBD104 expansion set. The libraries were then

176 sequenced on a MinION rev 4.1D using a R9.1 flowcell over 48 hours (Oxford
177 Nanopore Technologies, UK).
178
179 MinION data was basecalled using GPU-accelerated Guppy (V 3.1.5+781ed57) in
180 high accuracy mode. Adapters were confirmed and removed using Porechop (V
181 0.2.3_seqan2.1.1). Reads that had differential demultiplexing via Guppy and
182 Porechop were discarded, leaving only reads for which both programs had reached a
183 consensus. Chimeric reads were discarded using Unicycler's Scrub module (V 0.4.7).
184 Finally, reads were filtered using FiltLong (V 0.2.0), with parameters based on read
185 length and quality distributions generated by NanoPlot (V 1.24.0), removing relatively
186 short or low-quality reads (e.g. lower 10% of the distribution).
187
188 Circularised assemblies were produced using both the long and short read data by
189 Unicycler (V 0.4.7) (Wick et al., 2017). Following assembly, we ran additional rounds
190 of Pilon (V 1.23) until no further changes were found. Assemblies were annotated
191 using Prokka (V 1.13.3) (Seemann, 2014). Structural variants were identified using a
192 combination of Sniffles (V 1.0.12) and Assemblytics (V 1.0). Structural variants were
193 further filtered to high confidence calls by inspecting the BAM file and filtering to
194 discard minor allele variants (AF <0.9). Single nucleotide variants were called against
195 the hybrid assemblies using Snippy (V 4.3.6).
196
197 **Transcriptome sequencing**
198 RNA sequencing was performed on biological triplicates of the ancestral and
199 transconjugant strains. For each replicate, a colony was picked from overnight growth
200 on Nutrient Agar and added to 5 ml of Nutrient Broth (Sigma Aldrich, UK). Cultures
201 were incubated at 37˚C until reaching an OD600 of ~0.6. RNA was extracted using

202 Trizol (ThermoFisher, UK). Following isopropanol precipitation, DNA was digested
203 using Turbo DNAse (Thermofisher, UK) based on the manufacturer's protocol. The
204 final RNA solution was purified using a RNeasy Mini Kit (Qiagen, UK), and quantified
205 using a Qubit with the RNA HS assay kit. The RNA was immediately stored at -80˚C.
206
207 RNA sequencing was performed by the Centre for Genomics Research (Liverpool,
208 UK). The RNA integrity number and library insert size were verified using the Agilent
209 RNA 6000 Pico Kit and Bioanalyzer platform (Agilent, USA). The RiboZero (Illumina,
210 USA) kit was used to deplete rRNA, and dual indexed libraries were prepared using
211 the NEBNext Ultra Directional RNA sequencing kit (New England Biolabs, USA).
212 Libraries were sequenced on a HiSeq 4000 (Illumina, USA) configured to 2 x 150 bp
213 cycles. In order to obtain at least 10 million reads per sample, the sequencing run was
214 distributed across three lanes.
215
216 Kallisto (v 0.46.0) was used to quantify differential gene expression, with the high-
217 quality hybrid *de novo* assemblies of parental strains used as a reference. Input files
218 were prepared using Prokka (v 1.13.3) for annotation, genbank_to_kallisto.py
219 (https://github.com/AnnaSyme/genbank_to_kallisto.py) to convert the annotation files
220 for use with Kallisto, and GNU-Parallel (v 20180922) for job parallelisation. Differential
221 gene expression was analysed using Voom/Limma in Degust (V 3.20), with further
222 processing of the resulting differential counts in R (V 3.5.3). UPGMA clustering was
223 performed using DendroUPGMA (http://genomes.urv.cat/UPGMA/). Functional
224 categories were assigned to genes using eggnog-mapper (V 2).
225
226 **Plasmid persistence**

227 pLL35 encodes two TA systems and therefore is likely to be highly stable but this has
228 not been previously measured. To quantify the persistence of the plasmid over time,
229 4 replicate cultures of each plasmid-containing strain were propagated by daily serial
230 transfer in nutrient broth (NB) microcosms (6 ml of NB in a 30 ml glass universal vial)
231 for 16 days. 1% of each culture was transferred to fresh media every 24 hours.
232 Populations were plated out onto nutrient agar ± 4μg/ml of cefotaxime at days 0, 1, 2,
233 4, 7, 10, 13 and 16.
234
235 **Growth curves and phenotypic profiling**
236 Minimum inhibitory concentration (MIC) assays for the parental and transconjugant
237 strains were conducted according to the CLSI guidelines (CLSI, 2012), using nutrient
238 broth and cefotaxime. Static overnight cultures in 6 ml nutrient broth were established
239 from independent colonies previously grown on agar plates. The following day, 0.5
240 McFarland cell suspensions were prepared and further diluted 1/500 to inoculate 200
241 μl of nutrient broth in 96 well plates. The final cefotaxime concentrations tested were
242 0.25, 0.5, 0.75, 1, 1.25, 1.5, 1.75, and thereafter two-fold increases from 2 to 2,048
243 μg/ml, and the final volume per well was 200 μl (100 μl bacterial inoculum plus 100 μl
244 antibiotic solution). The OD600 was recorded after 24h of static incubation at 37 °C,
245 and normalised by subtracting the OD600 of a blank well. As working with positive
246 OD600 values facilitates further data analysis and interpretation, we linearly
247 transformed OD600 estimates by adding 0.0938876 to all data. For each strain and
248 plasmid combination, the relative growth at each antibiotic concentration was obtained
249 by dividing OD600 values in the presence of antibiotic by the OD600 of the
250 corresponding parental strain grown in the absence of antibiotic. The relative growth
251 values were used to calculate the area under the curve (AUC) with the auc function

252 from the R package flux (flux_0.3-0). Statistical analysis were performed on Box Cox
253 transformed data to fulfil ANOVA assumptions.
254
255 Growth kinetics for both plasmid-free and plasmid-containing strains were measured
256 using cultures grown in 200 µl nutrient broth per well in a 96 well plate using an
257 automated absorbance plate reader (Tecan Spark 10). Wells were inoculated using
258 the same procedure described above. Plates were incubated at 37 °C for 39 hours
259 and the optical density of each well was measured every 30 minutes at 600 nm, plates
260 were shaken for 5s (orbital shaking, movement amplitude 3mm, 180 rpm) and allowed
261 to settle for 50s prior to each reading. A humidity cassette was used to minimise
262 evaporation of the samples.
263
264 **Data availability**
265 Sequence data is available under bioproject PRJNA667580, and individual SRA
266 accessions are provided in Table S1.
267
268 **Results**
269
270 ***E. coli* strains varied in conjugational uptake of pLL35**
271 For most strains, the conjugation rate from *K. pneumoniae* was higher in static than in
272 shaken culture. Indeed, for several strains we detected no transconjugants from
273 shaken cultures in any of the replicates (e.g., F022 and F047 – ST131 clade A and C,
274 respectively), and only three strains consistently acquired the plasmid in both shaken
275 and static conditions (i.e., F037, F048, F054 – all ST131 clade B/C – Figure S1). Due
276 to the high number of missing replicates in shaken cultures, we were only able to

277 analyse variation across all strains in the conjugation rates estimated from static
278 cultures. In static cultures, strains varied in their ability to acquire the plasmid by
279 conjugation from *K. pneumoniae* (Figure S2; ANOVA, strain effect, $F_{7,36}$ = 19.23 P =
280 2.06e-10). Once acquired, however, the plasmid was stably maintained over time by
281 all strains (Figure S3; Wilcoxon test comparing population density averaged over time
282 on media with or without cefotaxime, all strains, P > 0.05).
283
284 **Strain-specific effects of pLL35 on resistance and bacterial growth kinetics.**
285 Plasmid acquisition increased resistance to cefotaxime but the level of resistance
286 conferred by the plasmid varied by strain (Figure 1; ANOVA, strain by plasmid
287 interaction, $F_{7, 32}$ = 2.968, P = 0.000219). Specifically, in strains F037, F047 and F054
288 the plasmid provided lower levels of cefotaxime resistance than in plasmid bearers of
289 the other strains.
290
291 Parental strains varied in their growth parameters (lag time, ANOVA, $F_{7, 32}$ = 5.358, P
292 = 0.000394; maximum growth rate, ANOVA, $F_{7, 32}$ = 6.3, P = 0.000108; saturation
293 density, ANOVA, $F_{7, 32}$ = 18.48, P = 0.00000000136; integral of the growth curve,
294 Kruskal-Wallis $\chi^2_7$ = 31.759, P = 0.000045). To control for this variation in baseline
295 growth among the strains, we normalised growth parameters per plasmid-carrying
296 strain by its corresponding parental strain. This gave estimates of relative growth
297 parameters, and thus of the impact of plasmid acquisition upon the growth of each
298 strain (i.e., a value of 1 would indicate no effect on growth of plasmid acquisition;
299 Figure 2). Strains varied in their relative maximum growth rate (ANOVA, $F_{7, 32}$ = 5.742,
300 P = 0.00023), relative saturation density (Kruskal-Wallis $\chi^2_7$ = 24.102, P = 0.001093),
301 and relative integral of the growth curve (ANOVA, $F_{7, 32}$ = 8.998, P = 0.00000424), but

302 not in their relative lag time (Kruskal-Wallis $\chi^2_7$ = 10.264, P = 0.1741). The clearest
303 impacts of plasmid acquisition on growth were apparent for the relative integral of the
304 growth curve (Figure 2), which is a useful measure of the overall effect of plasmid
305 acquisition on growth (Wright et al., 2018): The integral of the growth curve was
306 reduced by plasmid carriage in the strains GU15 and F047 (one-sample t-test of
307 relative integral against 1; GU15, t = 3.6933, df = 4, P = 0.021; F047, t = 4.1762, P =
308 0.014) but was increased in the strains F022 and F037 (one-sample t-test of relative
309 integral against 1; F022, t = 7.0987 df = 4 P = 0.0021; F037, t = 5.0836, P = 0.0071).
310 Thus, acquiring the ESBL plasmid had variable effects upon growth across the strains
311 causing both increased and decreased growth, whilst having a negligible impact upon
312 the growth of half of the strains tested.
313
314 Following the masking of any variants that occurred in the ancestral or control
315 sequence data, ESBL plasmid carriers contained very few SNPs, with the majority of
316 isolates containing no SNPs at all (n=6 out of 8). The position of detected SNPs was
317 determined, but no clear evidence of parallelism could be established (Table S2). To
318 confirm this limited genomic impact further, we sequenced three additional
319 independently constructed transconjugant replicates. This also revealed a small
320 number of SNPs (0-2 SNPs per replicate), with the majority of sequences containing
321 0 variants (n=16 out of 24).
322
323 **Strain specific transcriptional responses to acquisition of pLL35**
324 We next compared the transcriptomes of the pLL35 carrying transconjugants with their
325 parental strain to determine the effect of plasmid acquisition on host gene expression.
326 Combining differential gene expression analysis from three independent biological

327 replicates showed very little significant transcriptional response in any strain, with the
328 number of significantly (>2-fold log change) differentially expressed genes ranging
329 from 22 to zero at a false discovery rate (FDR) P-value of < 0.05 and 31 to zero at a
330 FDR P-value of < 0.1 (Figure S3). Volcano plots for the transcriptional impact of
331 plasmid acquisition per strain show highly strain-specific responses to acquisition of
332 pLL35, both in terms of the level of transcriptional response and the genes that were
333 differentially expressed (Figure 3). Strains ELU39, F104 and F037 showed no
334 significant changes in gene expression upon acquisition of the plasmid (at FDR P-
335 value of < 0.05 or < 0.1), strains GU15, F054 and F048 had fewer than 5 genes
336 significantly differentially expressed, and strains F022 and F047 showed between 10
337 and 22 genes significantly differentially expressed (at FDR P-value of < 0.05, Figure
338 S4). There was no correlation between magnitude of transcriptional response and the
339 growth responses observed in the strains (r = -0.6162, P = 0.1038).
340
341 **Functions whose expression was affected by pLL35 varied between strains**
342 We observed differences in the functions whose expression was significantly affected
343 by pLL35 acquisition between the strains. In F022 plasmid-carriers we observed
344 upregulation of the entire class 1, 2 and 3, flagella biosynthesis regulons relative to
345 the plasmid-free parental strain (Chilcott & Hughes, 2000). Further inspection of the
346 genome sequences of the parental and transconjugant F022 strains revealed that this
347 occurred due to an insertion of an IS1 family IS element in *lrhA,* the negative regulator
348 of *flhDC* (Figure 4).
349
350 In F047, pLL35 caused upregulation of a variety of chromosomal genes, including
351 those involved in various stress responses such as *cpxP* (envelope stress response),

352 *deaD* (low temperature response), *ibpAB* (heat and oxidative stress), and *soxS*
353 (superoxide stress master regulator). This is mirrored in several differentially
354 expressed genes just below the 2 log fold change significance threshold such as *dnaJ,*
355 *degP* and *osmY* (1.81, 1.64 1.59 FC), which are all involved in stress response. The
356 presence of plasmid also led to upregulation of *marR*, the repressor of the *mar*
357 antibiotic resistance and oxidative stress response regulon, though *marA* expression
358 was not significantly affected (1.0 FC, 0.57 FDR). Other functions upregulated by
359 plasmid acquisition included metabolic transport (*mgtA, pstS*) and anaerobic
360 metabolism genes (*glpD*).
361
362 In F048, several co-located hypothetical genes were upregulated in plasmid carriers,
363 3 of these were significantly upregulated while the remainder were slightly below the
364 FDR significance threshold. This region was further characterised with Prophage
365 Hunter, showing a putative ~60 Kb prophage. This prophage contains 78 genes and
366 shows 94% identity and 28% coverage with prophage CUS-3. No evidence of phage
367 mobilisation was detected by structural variant analysis, and the read depth at this
368 region (normalised to house-keeping genes) was consistent across both the parental
369 and transconjugant read sets suggesting that the observed upregulation was not due
370 to the presence of additional prophage copies.
371
372 In GU15, pLL35 led to down regulation of the entire sulfur biosynthesis and transport
373 operons (*cysA* – *cysW*). Significant downregulation was observed in *cysA* at FDR
374 >0.05, and *genes cysHIJKNWU* at FDR >0.1. The rest of the operon were expressed
375 at ranges slightly below the FDR significance threshold.
376

377 **Consistent pattern of low-level transcriptional response to pLL35**

378 Some genes known to be in operons or regulons did not pass significance threshold
379 in our FDR analysis, despite the rest of the operon or regulon doing so. This is due to
380 our use of amalgamated data from three independent biological replicates and strict
381 significance thresholds. We decided to further analyse the expression of all core genes
382 (Figure S5) using a principal component analysis to detect genes that were
383 differentially expressed across our host range (Figure S6). Analysis of this set of genes
384 showed some consistent patterns of differential expression across all strains. A
385 common pattern of upregulation in response to acquisition of pLL35 was observed for
386 the *cit* operon, *his* operon, the *hya, hyb,* and *hyc* operon, and the *nar* and *ttd* operons
387 and the *gad* loci (Figure 5). Conversely, there was a common pattern of down-
388 regulation in response to acquisition of pLL35 of the *csg, gat, waa, yad,* and *yih*
389 operons across all strains. Functional enrichment analysis of genes in the 5$^{th}$ and 95$^{th}$
390 percentile of these differentially expressed loci confirmed this consistent fine-scale
391 transcriptional response to the plasmid in genes associated with the cell wall, signal
392 transduction, cell motility, energy production and conversion, and carbohydrate
393 transport and metabolism (Figure 5).

394

395 **Discussion**

396 Evidence from experimental evolution studies has provided us with a detailed picture
397 of the impact that acquisition of plasmids and their stable integration into a host cells
398 genetic inventory has on cell fitness (Brockhurst et al., 2019). Much of this fitness
399 impact is driven by changes in transcription in the acquiring cell, both the need to
400 transcribe genes on the plasmid, but also global effects on host cell transcription to
401 offset the impact of carrying the plasmid (Buckner et al., 2018; Harrison et al., 2015;

402 Millan et al., 2015). There are very few of these studies examining the impact of
403 acquisition of multi-drug resistance plasmids on cells from genetically diverse strains
404 (Buckner et al., 2018), with most evidence of adaptations that occur as a result of MDR
405 plasmid acquisition stemming from large comparative population genomics studies
406 (Feng et al., 2019; McNally et al., 2016, 2019). Here we address this by examining the
407 impact of acquisition of an MDR plasmid on *E. coli* from a variety of genetic
408 backgrounds ranging from environmental lineages with no reported MDR plasmid
409 carriage to MDR-plasmid-free clinical isolates from the ST131 lineage most commonly
410 associated with multi-drug resistance in clinical settings.
411
412 Acquisition of the ESBL plasmid, pLL35, varied among strains, with some strains
413 unable to successfully conjugate under shaking conditions. All strains stably
414 maintained the plasmid once they had acquired it, likely due to the presence of two
415 toxin-antitoxin systems on pLL35. Plasmid acquisition had variable effects on growth
416 between strains. Notably, plasmid acquisition was not costly in terms of relative growth
417 for all the strains, with increased growth of plasmid carriers relative to their parentals
418 observed in two strains. This is surprising given that plasmid acquisition has been
419 shown to be associated with fitness costs across a diversity of plasmid-host
420 interactions, although variation in the magnitude of the cost has been described
421 (Bouma & Lenski, 1988; Göttig et al., 2016; Kottara et al., 2018; Nang et al., 2018).
422 However, our data are consistent with those of another recent study that tested the
423 fitness effect of a given plasmid across the range of genetic backgrounds present in a
424 host species. Like ours, this study revealed diverse fitness impacts ranging across a
425 continuum from costly to beneficial (Alonso-del Valle et al., 2020). These data highlight
426 that the fitness effects of a plasmid can be highly strain-specific, and thus are likely to

427 arise from specific genetic interactions rather than the generic biosynthetic costs of
428 plasmid maintenance. Interestingly, effects on growth of plasmid acquisition were
429 uncorrelated with the extent of changes in gene expression across the strains,
430 suggesting that greater plasmid-mediated gene dysregulation does not necessarily
431 translate to larger fitness costs.
432
433 Strains varied in the level of cefotaxime resistance provided by the ESBL plasmid.
434 This suggests epistasis between the plasmid ESBL gene and chromosomal loci that
435 vary among strains. Through comparison of the strain genomes we could not identify
436 any clear differences in chromosomal gene content among strains in terms of known
437 resistance determinants to explain the observed variation in cefotaxime resistance.
438 For example, all strains encode the same set of standard efflux pumps with the
439 exception of F047 and F048, which also contain *tetA*. Yet F047 and F048 differ
440 markedly to each other in their cefotaxime resistance response, suggesting that TetA
441 does not explain the variable resistance response. All strains encode a variant of
442 *blaEC*. In addition, F022 and F047 encode *blaTEM-1* but vary in their cefotaxime
443 resistance response, suggesting that *blaTEM-1* does not explain the variable
444 resistance response. This is perhaps unsurprising as the prediction of a strain's
445 resistance phenotype from gene content alone is notoriously inaccurate (Mahfouz et
446 al., 2020).
447
448 Comparing the transcriptomes of plasmid-carriers with their parental strain revealed
449 highly strain-specific effects of plasmid acquisition on the expression of chromosomal
450 genes. The number of genes whose transcription was affected by the plasmid was
451 small in all strains, ranging from 0 to just 22 genes (at FDR < 0.05). These data stand

452 in contrast to other studies where the expression levels of hundreds of chromosomal
453 genes are affected by plasmid acquisition (Harrison et al., 2015; Long et al., 2019;
454 Millan et al., 2015; Takahashi et al., 2015). Significant transcriptional effects of ESBL
455 plasmid acquisition were focussed in discrete operons or regulons. For example, in
456 GU15 we observed down-regulation of the sulfur biosynthesis and transport operons
457 (*cysA* – *cysW*). In F048 plasmid-carriers, flavohaemoglobin (Hmp), which is
458 responsible for resistance to nitrosative stress (Stevanin et al., 2007), was upregulated
459 following plasmid acquisition. In F047, the transcriptional impact of plasmid acquisition
460 was more widespread, affecting more diverse functions, but, consistent with F048,
461 most of these were related to stress-responses. Upregulation was observed in *marR*,
462 which did not extend to *marA*; *marA* has been demonstrated to have a short half-life
463 (3 minutes) and is quickly depleted when the environmental stress is removed (Vinué
464 et al., 2013). Increased expression was also observed in heat shock proteins IbpA/B.
465 The function of IbpA/B extends beyond heat stress; previous studies have shown that
466 increased *ibpA/B* expression resulted in the overproduction of a beta-lactamase
467 precursor, potentially through IbpA/B binding to the precursor protein, preventing
468 subsequent processing (Kuczyńska-Wiśnik et al., 2002). This could explain the
469 lowered cefotaxime MIC observed, though the exact cause of *ibpA/B* upregulation is
470 unclear. All of these factors indicate that F047 exhibited a strong stress response to
471 acquisition of the plasmid. Plasmids are known to elicit stress responses in their host
472 cells (San Millan et al., 2018), for example through the conjugation-mediated cell
473 envelope stress in *E. coli* (Yang et al., 2008), or due to single stranded DNA activating
474 the SOS response (Baharoglu et al., 2010). Additionally, pLL35 encodes DNA
475 polymerase V genes *umuDC,* the chromosomal homologs of which are part of the
476 SOS response regulon (Cohen et al., 2008; Fernández De Henestrosa et al., 2000).

477 Intriguingly, a plasmid-encoded *umuD* gene has previously been shown to regulate
478 the SOS response in *Pseudomonas aeruginosa* (Díaz-Magaña et al., 2015),
479 suggesting that plasmids may directly manipulate expression of the bacterial SOS
480 response. It is hypothesised the production of conjugation apparatus may lead to
481 misfolded proteins; F047 failed to conjugate in shaking conditions. This may be due to
482 an increase in the concentration of damaged or misfolded proteins beyond that which
483 would be mitigated by increased expression of stress response proteins (e.g. DegP,
484 CpxP).
485
486 In two of our strains there is evidence of a transcriptional response possibly driven by
487 the relationship between mobile genetic elements. In F022, the upregulation of
488 flagellar and chemotaxis genes was explained by a 768 bp insertion of an IS1 family
489 element encoding both *insA* and *insB* in the *lrhA* regulator. LrhA belongs to the lysR
490 family and binds to and negatively regulates expression of the *flhDC* master regulator.
491 Truncation of *lrhA* is therefore likely to have prevented negative regulation of *flhDC*,
492 leading to uncontrolled expression of the flagellar and chemotaxis operons. Genomic
493 comparison of IS elements within the F022 genome revealed 7 identical IS1
494 sequences in the parental genome, with 4 found on the chromosome, and 3 on a
495 canonical plasmid. Upon plasmid acquisition, this element inserted one additional
496 time. This appeared to be a random event, as a similar insertion could not be detected
497 in the short-read data of replicate transconjugants. In F048 a set of co-located
498 upregulated genes were associated with a chromosomal prophage. Many prophages
499 respond to host stress responses, which can be induced by plasmid acquisition and
500 thus may explain the upregulation of prophage gene expression observed here.

501 Prophages have also been shown to excise and replicate under stress conditions, but
502 we did not detect any excision or genomic amplification of the phage region.
503
504 Besides those genes whose expression was significantly altered by ESBL plasmid
505 acquisition (i.e. that met the stringent significance threshold), we also observed a
506 subtle but consistent transcriptional response to plasmid acquisition among all genes
507 with a >2-fold log change in expression. Upon acquisition of a plasmid the most
508 intuitive scenario would be a fall in chromosomal transcription as transcriptional
509 machinery is sequestered at plasmid promoters (Dunn et al., 2019). Accordingly,
510 across all strains, we observed reduction in transcription of *csg* genes encoding curli
511 fimbriae and genes involved in cell wall and outer membrane production including the
512 *waa* LPS core genes. These genes are involved in biosynthesis of energetically costly
513 structures in the cell and their repression is consistent with offsetting energetic costs
514 of plasmid maintenance. Conversely, we observed consistently increased
515 transcription of *hya, hyb, hyc* genes encoding the hydrogenase-1 and 3 complexes,
516 the *nar* gene encoding nitrate reductase, the *ttr* gene encoding tartrate dehydratase,
517 and the *gad* glutamate decarboxylase operon. All of these genes are involved in
518 various aspects of anaerobic metabolism, which is known to be important for
519 colonising the mammalian gut. Moreover, some of these genes exhibit negative
520 frequency dependent selection in the MDR clade C of *E. coli* ST131, which may reflect
521 selection for enhanced intestinal colonisation (McNally et al., 2019). The observation
522 of broad-scale, subtle changes to chromosomal gene expression caused by an MDR
523 plasmid that are consistent across diverse bacterial lineages warrants further
524 investigation. Their scale is suggestive of a role for plasmid-encoded regulatory

525 elements, such as small RNAs (Vial & Hommais, 2020), with the potential for genome-
526 wide effects.
527
528 **Conclusion**
529 We observed strain-specific but limited effects of acquisition of an ESBL plasmid
530 across diverse *E. coli* lineages. The transcriptional response to plasmid acquisition
531 was limited to differential expression of small numbers of genes within discrete
532 operons or regulons whose identity varied between strains. More subtle but consistent
533 effects of plasmid acquisition on global transcription were observed, affecting a range
534 of cellular processes. Relative growth and cefotaxime resistance of ESBL plasmid
535 carriers varied between strains. Overall, our findings suggest that the effects of MDR
536 plasmid acquisition upon the host cell arise from specific genetic interactions that are
537 likely to be difficult to predict a priori and that fitness costs are unlikely to act as a
538 barrier to transmission of this MDR plasmid in natural populations of *E. coli*.
539
540 **Acknowledgements**
541 This work was funded by a BBSRC project grant [BB/R006261/1 & BB/R006253/1]
542 jointly awarded to AM and MB respectively.
543
544 **Figures**
545 **Figure 1 – The level of resistance to cefotaxime conferred by the pLL35 varied**
546 **by strain.** Plots are facetted by *E. coli* strain. Solid lines show the mean (n=3) ±
547 standard error of relative growth measured using optical density (OD) at 600 nm with
548 (red) or without (blue) pLL35 across gradients of increasing cefotaxime concentration.
549 Horizontal dashed lines indicate a relative growth value of 0.5, i.e., the $MIC_{50}$.

550

551

552 **Figure 2 – The effect of acquiring pLL35 on bacterial growth kinetics varied by**
553 **strain.** Panels show the response of the following growth parameters to plasmid
554 acquisition: (A) lag time, (B) maximum growth rate, (C) maximum density, and (D)
555 integral (i.e. area under the growth curve). Boxes show normalised values (plasmid-
556 carrying strain value divided by parental strain value) for each strain (n=5) indicating
557 the performance of plasmid carriers relative to their parental strain where a value of 1
558 represents equal performance. The lower hinge of the box denotes the $25^{th}$ percentile,
559 the upper hinge denotes the $75^{th}$ percentile, and the line within the box indicates the
560 median. Upper whiskers extend to the highest value no further than 1.5 times the inter-
561 quartile range from the hinge. Lower whiskers extend to the smallest value no further
562 than 1.5 times the inter-quartile range from the hinge. Points indicate outliers beyond
563 the whiskers.

564

565 **Figure 3 – Transcriptional responses to acquiring pLL35 varied by strain.** $Log_2$
566 fold change (CTX) of differentially expression data and their statistical significance (-
567 $log_{10}$ of the P-value). Whilst 4 of the 8 isolates showed no significant transcriptional
568 differences, other isolates showed patterns of differential expression in discrete
569 operons, or in genes under the control of a common regulator. The transcriptomic
570 effects observed in this host range are determined by strain, rather than host genetic
571 background. Blue = Significant Fold Change (>2) OR Significant P value (<0.05), Red
572 = Also FDR Significant at a threshold of <0.10, Green = Also FDR Significant at a
573 threshold of <0.05, Black = Not significant.

574

575 **Figure 4 – Transcriptional response of strain F022 was likely caused by a**
576 **chromosomal insertion of an IS element.** A) Parental genome sequence with fully
577 intact *lrhA* gene. B) Transconjugant genome sequence with an IS1 family transposase
578 sequence causing a truncation to lrhA. C) IS1 family transposase with left and right
579 inverted repeat sequences, and a 9 base pair target site duplication. This particular
580 IS1 occurs 7 times in the parental strain, and has inserted one additional time upon
581 plasmid conjugation. Querying the ISfinder database shows that this IS1 shares 97%
582 sequence identity with IS1 R, B and D. This element encodes two ORFs, *insA* and
583 *insB*. D) Depth of long reads uniquely mapped to the transconjugant assembly. The
584 minimum depth of reads that were successfully mapped to this region is 50, and in the
585 parental isolate there are 0 reads that map to the IS1 transposase.
586
587 **Figure 5 – Transcriptional change of genes from the extremes of the PCA**
588 **distribution show some common signatures of differential expression** (e.g. *cit*
589 operon, *his* operon, the *hya, hyb,* and *hyc* operon, and the *nar*, *gad* and *ttd* operons).
590 Genes were extracted from the 5$^{th}$ and 95$^{th}$ percentile of the PCA distribution from
591 figure S6 (i.e. genes extraneous to the central distribution). These genes were
592 assigned to COGS functional categories, with each category ordered via UPGMA
593 clustering of the expression data.
594
595 **Supplementary Material**
596 **Figure S1** – CTX-M-15 containing plasmid pLL35. A) Genomic map of pLL35 showing
597 a complete transfer region including a full suite of conjugation machine (tra locus), and
598 a complex antibiotic resistance region that confers resistance to cephalosporins,
599 aminogylcosides and quinolones. Within this region, OXA-9 is found to contain a

600 premature stop codon. pLL35 was found to contain a novel IS element flanked by a 5
601 bp terminal site duplication (TCCTG). B) Schematic of the resistance region, which
602 contains Tn1331b that is interrupted by a 2971 bp insertion of ISEcp1 containing a
603 1315 bp passenger section that includes CTX-M-15.
604
605 **Figure S2** – Conjugational uptake of pLL35 varied with *E. coli* strain and culturing
606 conditions. Open symbols show mean ± standard error of $\log_{10}$ conjugation rate for
607 each strain and culturing condition. Colour denotes culturing condition (shaken culture
608 = green; static culture = orange). Individual replicate values are shown as different
609 symbol shapes. Symbols are jittered to prevent over-plotting.
610
611
612 **Figure S3** – **Stable maintenance of pLL35 in all *E. coli* strains.** Plots are facetted
613 horizontally by strain. Lines show the mean (n=4) ± standard error (shaded area)
614 bacterial population densities over time from colony forming unit counts on nutrient
615 agar plates to give the whole population (blue) or nutrient agar plates supplemented
616 with 4 µg/ml of cefotaxime to give the plasmid-carrier fraction of the population (red).
617
618 **Figure S4** – **The magnitude of the transcriptional response to pLL35 acquisition**
619 **varied by strain.** A) Number of genes that were significantly (FDR <0.05) differentially
620 expressed (>2 log fold change). B) Number of genes that were significantly (FDR
621 <0.10) differentially expressed (>2 log fold change). Red = number of genes
622 upregulated, Blue = number of genes that were downregulated.
623

624 **Figure S5 – Global transcriptional response of ~779 core genes across all**
625 **strains, sorted by functional cog category.** Gene order is determined via UPGMA
626 clustering of log2 transcriptional changes. A = Cellular processes and signalling, B =
627 Metabolism , C = Information storage and processing, D = Poorly characterised. The
628 isolates vary in their transcriptional response to the plasmid in a strain dependent
629 manner, however a large number of metabolism genes can be seen to increase in
630 transcription across all strains. Isolate F022, belonging to ST-131 Clade A -which is
631 not typically associated with MDR plasmids – exhibits the most disparate differential
632 expression profile.
633
634 **Figure S6 – PCA distributions of expression values from functionally**
635 **categorised core genes.** A = Cellular processes and signalling, B = Metabolism , C
636 = Information storage and processing. D shows how each isolate is contributing to the
637 PCA distribution. This data highlights which genes exhibit the greatest level of
638 differential expression amongst the isolates, with several candidates in each larger
639 COG category. Panel D recapitulates the phylogenetic relatedness of isolates, with
640 environmental isolates, MDR associated and non-associated lineages appearing
641 together.
642
643 **Table S1** – Accession numbers for all read data associated with this study.
644
645 **Table S2** – Variants detected in transconjugant strains and their impact on host
646 transcription, and variants detected in independent conjugation replicates. Positions
647 highlighted in bold occur in multiple replicates.
648

649
650 **References**


651 Alonso-del Valle, A., León-Sampedro, R., Rodríguez-Beltrán, J., Hernández-García,
652 M., Ruiz-Garbajosa, P., Cantón, R., San Millán, Á., Spain, M., & Peña-Miller, R.
653 (2020). The distribution of plasmid fitness effects explains plasmid persistence
654 in bacterial. *BioRxiv*, 2020.08.01.230672.
655 https://doi.org/10.1101/2020.08.01.230672

656 Baharoglu, Z., Bikard, D., & Mazel, D. (2010). Conjugative DNA transfer induces the
657 bacterial SOS response and promotes antibiotic resistance development
658 through integron activation. *PLoS Genetics*.
659 https://doi.org/10.1371/journal.pgen.1001165

660 Banerjee, R., & Johnson, J. R. (2014). A New Clone Sweeps Clean: the Enigmatic
661 Emergence of Escherichia coli Sequence Type 131. *Antimicrobial Agents and*
662 *Chemotherapy*, *58*(9), 4997–5004. https://doi.org/10.1128/AAC.02824-14

663 Bouma, J. E., & Lenski, R. E. (1988). Evolution of a bacteria/plasmid association.
664 *Nature*, *335*(6188), 351–352. https://doi.org/10.1038/335351a0

665 Brockhurst, M. A., Harrison, E., Hall, J. P. J., Richards, T., McNally, A., & MacLean,
666 C. (2019). The Ecology and Evolution of Pangenomes. *Current Biology : CB*,
667 *29*(20), R1094–R1103. https://doi.org/10.1016/j.cub.2019.08.012

668 Buckner, M. M. C., Saw, H. T. H., Osagie, R. N., McNally, A., Ricci, V., Wand, M. E.,
669 Woodford, N., Ivens, A., Webber, M. A., & Piddock, L. J. V. (2018). Clinically
670 Relevant Plasmid-Host Interactions Indicate that Transcriptional and Not
671 Genomic Modifications Ameliorate Fitness Costs of Klebsiella pneumoniae
672 Carbapenemase-Carrying Plasmids. *MBio*, *9*(2).
673 https://doi.org/10.1128/mBio.02303-17

674 Chilcott, G. S., & Hughes, K. T. (2000). Coupling of flagellar gene expression to

flagellar assembly in Salmonella enterica serovar typhimurium and Escherichia coli. *Microbiology and Molecular Biology Reviews : MMBR*, *64*(4), 694–708. https://doi.org/10.1128/mmbr.64.4.694-708.2000

CLSI. (2012). *Methods for Dilution Antimicrobial Test for Bacteria that Grow Aerobically. M7-A*. Wayne, PA.

Cohen, S. E., Foti, J. J., Simmons, L. A., & Walker, G. C. (2008). The SOS Regulatory Network. *EcoSal Plus*, *3*(1). https://doi.org/10.1128/ecosalplus.5.4.3

Díaz-Magaña, A., Alva-Murillo, N., Chávez-Moctezuma, M. P., López-Meza, J. E., Ramírez-Díaz, M. I., & Cervantes, C. (2015). A plasmid-encoded UmuD homologue regulates expression of pseudomonas aeruginosa SOS genes. *Microbiology (United Kingdom)*, *161*(7), 1516–1523. https://doi.org/10.1099/mic.0.000103

Dunn, S. J., Connor, C., & McNally, A. (2019). The evolution and transmission of multi-drug resistant Escherichia coli and Klebsiella pneumoniae: the complexity of clones and plasmids. In *Current Opinion in Microbiology* (Vol. 51, pp. 51–56). https://doi.org/10.1016/j.mib.2019.06.004

Feng, Y., Liu, L., Lin, J., Ma, K., Long, H., Wei, L., Xie, Y., McNally, A., & Zong, Z. (2019). Key evolutionary events in the emergence of a globally disseminated, carbapenem resistant clone in the Escherichia coli ST410 lineage. *Communications Biology*, *2*, 322. https://doi.org/10.1038/s42003-019-0569-1

Fernández De Henestrosa, A. R., Ogi, T., Aoyagi, S., Chafin, D., Hayes, J. J., Ohmori, H., & Woodgate, R. (2000). Identification of additional genes belonging to the LexA regulon in Escherichia coli. *Molecular Microbiology*, *35*(6), 1560–1572. https://doi.org/10.1046/j.1365-2958.2000.01826.x

Göttig, S., Riedel-Christ, S., Saleh, A., Kempf, V. A. J., & Hamprecht, A. (2016).

Impact of blaNDM-1 on fitness and pathogenicity of Escherichia coli and Klebsiella pneumoniae. *International Journal of Antimicrobial Agents*, *47*(6), 430–435. https://doi.org/10.1016/j.ijantimicag.2016.02.019

Harrison, E., Guymer, D., Spiers, A. J., Paterson, S., & Brockhurst, M. A. (2015). Parallel Compensatory Evolution Stabilizes Plasmids across the Parasitism-Mutualism Continuum. *Current Biology*, *25*(15), 2034–2039. https://doi.org/10.1016/j.cub.2015.06.024

Kottara, A., Hall, J. P. J., Harrison, E., & Brockhurst, M. A. (2018). Variable plasmid fitness effects and mobile genetic element dynamics across Pseudomonas species. *FEMS Microbiology Ecology*, *94*(1), 172. https://doi.org/10.1093/femsec/fix172

Kuczyńska-Wiśnik, D., Kędzierska, S., Matuszewska, E., Lund, P., Taylor, A., Lipińska, B., & Laskowska, E. (2002). The Escherichia coli small heat-shock proteins IbpA and IbpB prevent the aggregation of endogenous proteins denatured in vivo during extreme heat shock. *Microbiology*, *148*(6), 1757–1765. https://doi.org/10.1099/00221287-148-6-1757

Long, D., Zhu, L. L., Du, F. L., Xiang, T. X., Wan, L. G., Wei, D. D., Zhang, W., & Liu, Y. (2019). Phenotypical profile and global transcriptomic profile of Hypervirulent Klebsiella pneumoniae due to carbapenemase-encoding plasmid acquisition. *BMC Genomics*, *20*(1), 480. https://doi.org/10.1186/s12864-019-5705-2

Mahfouz, N., Ferreira, I., Beisken, S., von Haeseler, A., & Posch, A. E. (2020). Large-scale assessment of antimicrobial resistance marker databases for genetic phenotype prediction: a systematic review. *Journal of Antimicrobial Chemotherapy*. https://doi.org/10.1093/jac/dkaa257

Mathers, A. J., Peirano, G., & Pitout, J. D. D. (2015). The role of epidemic resistance

725 plasmids and international high-risk clones in the spread of multidrug-resistant
726 Enterobacteriaceae. *Clinical Microbiology Reviews*, *28*(3), 565–591.
727 https://doi.org/10.1128/CMR.00116-14
728 McNally, A., Kallonen, T., Connor, C., Abudahab, K., Aanensen, D. M., Horner, C.,
729 Peacock, S. J., Parkhill, J., Croucher, N. J., & Corander, J. (2019).
730 Diversification of Colonization Factors in a Multidrug-Resistant Escherichia coli
731 Lineage Evolving under Negative Frequency-Dependent Selection. *MBio*, *10*(2).
732 https://doi.org/10.1128/mBio.00644-19
733 McNally, A., Oren, Y., Kelly, D., Pascoe, B., Dunn, S., Sreecharan, T., Vehkala, M.,
734 Välimäki, N., Prentice, M. B., Ashour, A., Avram, O., Pupko, T., Dobrindt, U.,
735 Literak, I., Guenther, S., Schaufler, K., Wieler, L. H., Zhiyong, Z., Sheppard, S.
736 K., … Corander, J. (2016). Combined Analysis of Variation in Core, Accessory
737 and Regulatory Genome Regions Provides a Super-Resolution View into the
738 Evolution of Bacterial Populations. *PLoS Genetics*, *12*(9), e1006280.
739 https://doi.org/10.1371/journal.pgen.1006280
740 Millan, A. S., Toll-Riera, M., Qi, Q., & MacLean, R. C. (2015). Interactions between
741 horizontally acquired genes create a fitness cost in Pseudomonas aeruginosa.
742 *Nature Communications*, *6*. https://doi.org/10.1038/ncomms7845
743 Nang, S. C., Morris, F. C., McDonald, M. J., Han, M. L., Wang, J., Strugnell, R. A.,
744 Velkov, T., & Li, J. (2018). Fitness cost of mcr-1-mediated polymyxin resistance
745 in Klebsiella pneumoniae. *Journal of Antimicrobial Chemotherapy*, *73*(6), 1604–
746 1610. https://doi.org/10.1093/jac/dky061
747 Peirano, G., Schreckenberger, P. C., & Pitout, J. D. D. (2011). Characteristics of
748 NDM-1-Producing Escherichia coli Isolates That Belong to the Successful and
749 Virulent Clone ST131. *Antimicrobial Agents and Chemotherapy*, *55*(6), 2986–

2988.

Petty, N. K., Zakour, N. L. Ben, Stanton-Cook, M., Skippington, E., Totsika, M., Forde, B. M., Phan, M. D., Moriel, D. G., Peters, K. M., Davies, M., Rogers, B. A., Dougan, G., Rodriguez-Baño, J., Pascual, A., Pitout, J. D., Upton, M., Paterson, D. L., Walsh, T. R., Schembri, M. A., & Beatson, S. A. (2014). Global dissemination of a multidrug resistant Escherichia coli clone. *Proc Natl Acad Sci U S A*, *doi/10.107*.

Sambrook, J., & Russell, D. W. (2006). Purification of Nucleic Acids by Extraction with Phenol:Chloroform. *Cold Spring Harbor Protocols*. https://doi.org/10.1101/pdb.prot4455

San Millan, A., Toll-Riera, M., Qi, Q., Betts, A., Hopkinson, R. J., McCullagh, J., & MacLean, R. C. (2018). Integrative analysis of fitness and metabolic effects of plasmids in Pseudomonas aeruginosa PAO1. *The ISME Journal*, *12*(12), 3014–3024. https://doi.org/10.1038/s41396-018-0224-8

Seemann, T. (2014). Prokka: rapid prokaryotic genome annotation. *Bioinformatics*, *30*(14), 2068–2069. https://doi.org/10.1093/bioinformatics/btu153

Simonsen, L., Gordon, D. M., Stewart, F. M., & Levin, B. R. (1990). Estimating the rate of plasmid transfer: An end-point method. *Journal of General Microbiology*, *136*(11), 2319–2325. https://doi.org/10.1099/00221287-136-11-2319

Stevanin, T. M., Read, R. C., & Poole, R. K. (2007). The hmp gene encoding the NO-inducible flavohaemoglobin in Escherichia coli confers a protective advantage in resisting killing within macrophages, but not in vitro: Links with swarming motility. *Gene*, *398*(1-2 SPEC. ISS.), 62–68. https://doi.org/10.1016/j.gene.2007.03.021

Takahashi, Y., Shintani, M., Takase, N., Kazo, Y., Kawamura, F., Hara, H., Nishida,

775 H., Okada, K., Yamane, H., & Nojiri, H. (2015). Modulation of primary cell
776 function of host Pseudomonas bacteria by the conjugative plasmid pCAR1.
777 *Environmental Microbiology*, *17*(1), 134–155. https://doi.org/10.1111/1462-
778 2920.12515
779 Vial, L., & Hommais, F. (2020). Plasmid-chromosome cross-talks. *Environmental*
780 *Microbiology*, *22*(2), 540–556. https://doi.org/10.1111/1462-2920.14880
781 Vinué, L., Mcmurry, L. M., & Levy, S. B. (2013). The 216-bp marB gene of the
782 marRAB operon in Escherichia coli encodes a periplasmic protein which
783 reduces the transcription rate of marA. *FEMS Microbiology Letters*.
784 https://doi.org/10.1111/1574-6968.12182
785 Wick, R. R., Judd, L. M., Gorrie, C. L., & Holt, K. E. (2017). Unicycler: Resolving
786 bacterial genome assemblies from short and long sequencing reads. *PLoS*
787 *Computational Biology*, *13*(6), e1005595.
788 https://doi.org/10.1371/journal.pcbi.1005595
789 Wright, R. C. T., Friman, V.-P., Smith, M. C. M., & Brockhurst, M. A. (2018). Cross-
790 resistance is modular in bacteria-phage interactions. *PLoS Biology*, *16*(10),
791 e2006057. https://doi.org/10.1371/journal.pbio.2006057
792 Wu, W., Feng, Y., Tang, G., Qiao, F., McNally, A., & Zong, Z. (2019). NDM Metallo-
793 beta-Lactamases and Their Bacterial Producers in Health Care Settings. *Clinical*
794 *Microbiology Reviews*, *32*(2). https://doi.org/10.1128/CMR.00115-18
795 Yang, X., Ma, Q., & Wood, T. K. (2008). The R1 conjugative plasmid increases
796 Escherichia coli biofilm formation through an envelope stress response. *Applied*
797 *and Environmental Microbiology*, *74*(9), 2690–2699.
798 https://doi.org/10.1128/AEM.02809-07
799 Zong, Z., Fenn, S., Connor, C., Feng, Y., & McNally, A. (2018). Complete genomic

characterization of two Escherichia coli lineages responsible for a cluster of carbapenem-resistant infections in a Chinese hospital. *Journal of Antimicrobial Chemotherapy*, *73*(9), 2340–2346. https://doi.org/10.1093/jac/dky210

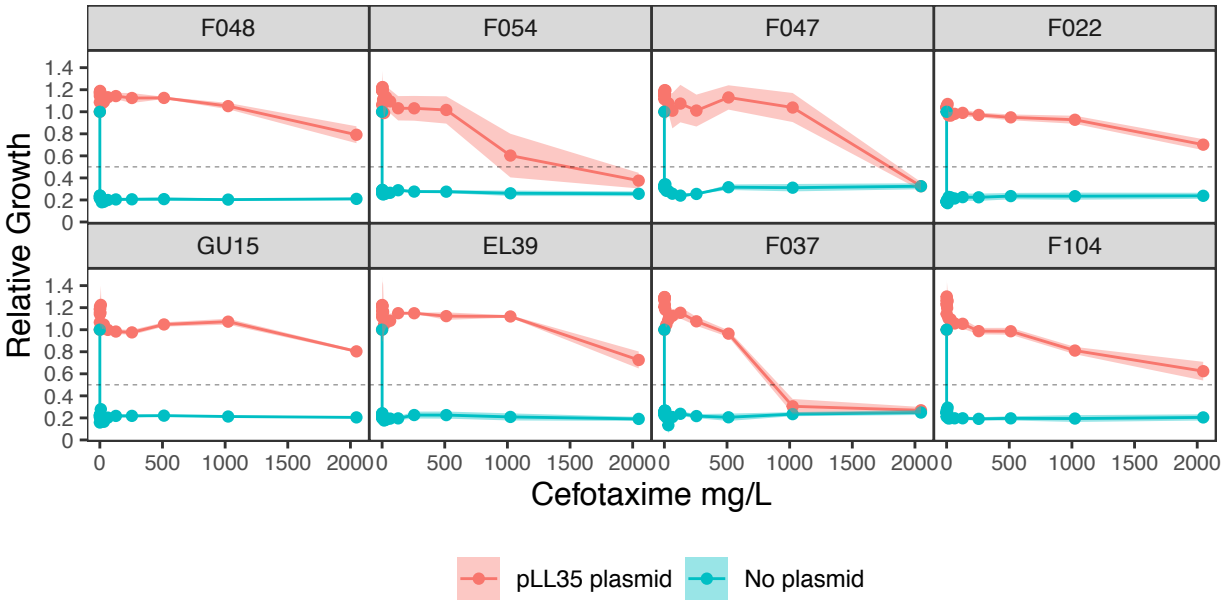

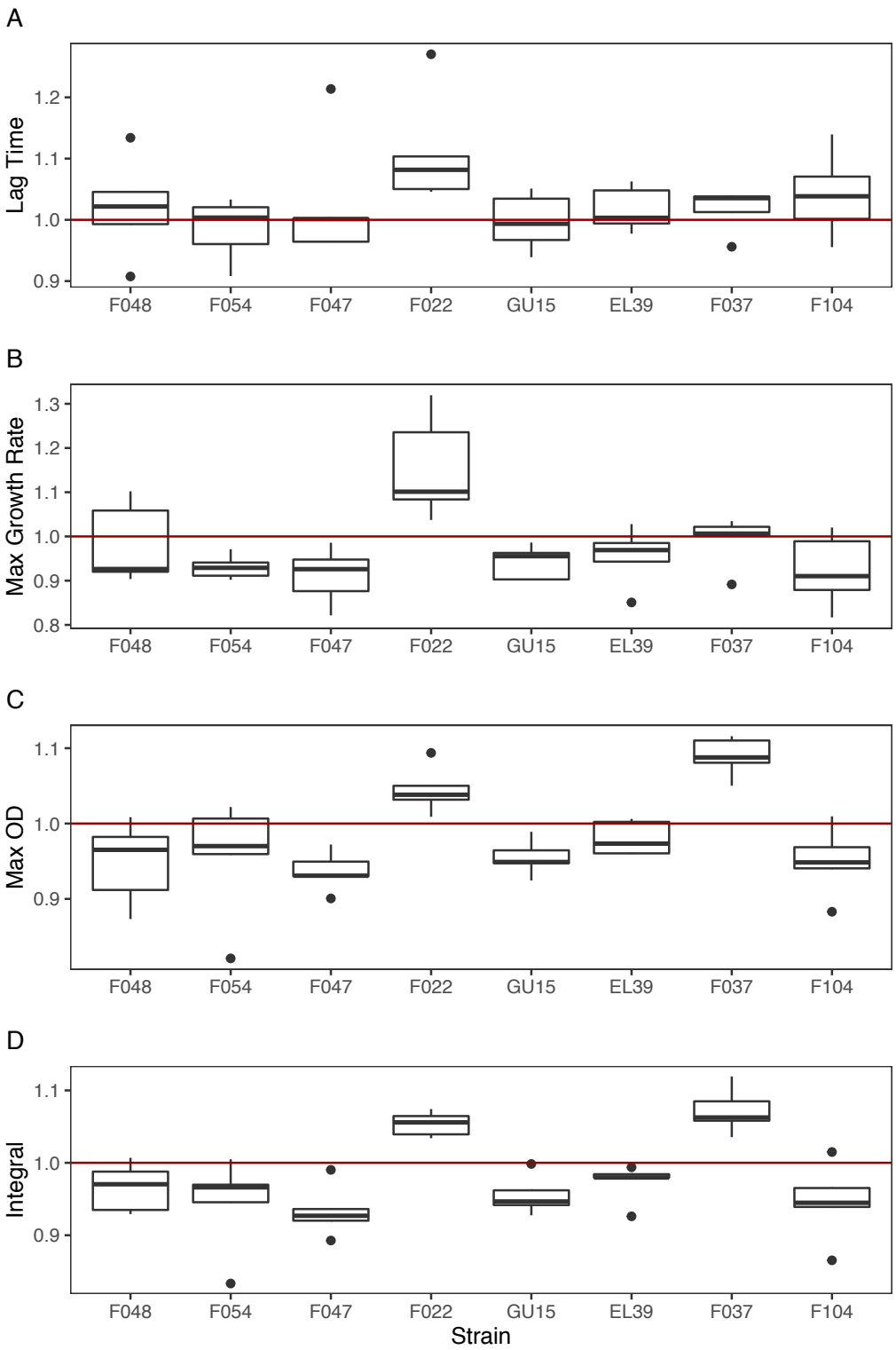
A
Lag Time
1.2
1.1
1.0
0.9
F048
F054
F047
F022
GU15
EL39
F037
F104
B
Max Growth Rate
1.3
1.2
1.1
1.0
0.9
0.8
C
Max OD
1.1
1.0
0.9
D
Integral
Strain

806

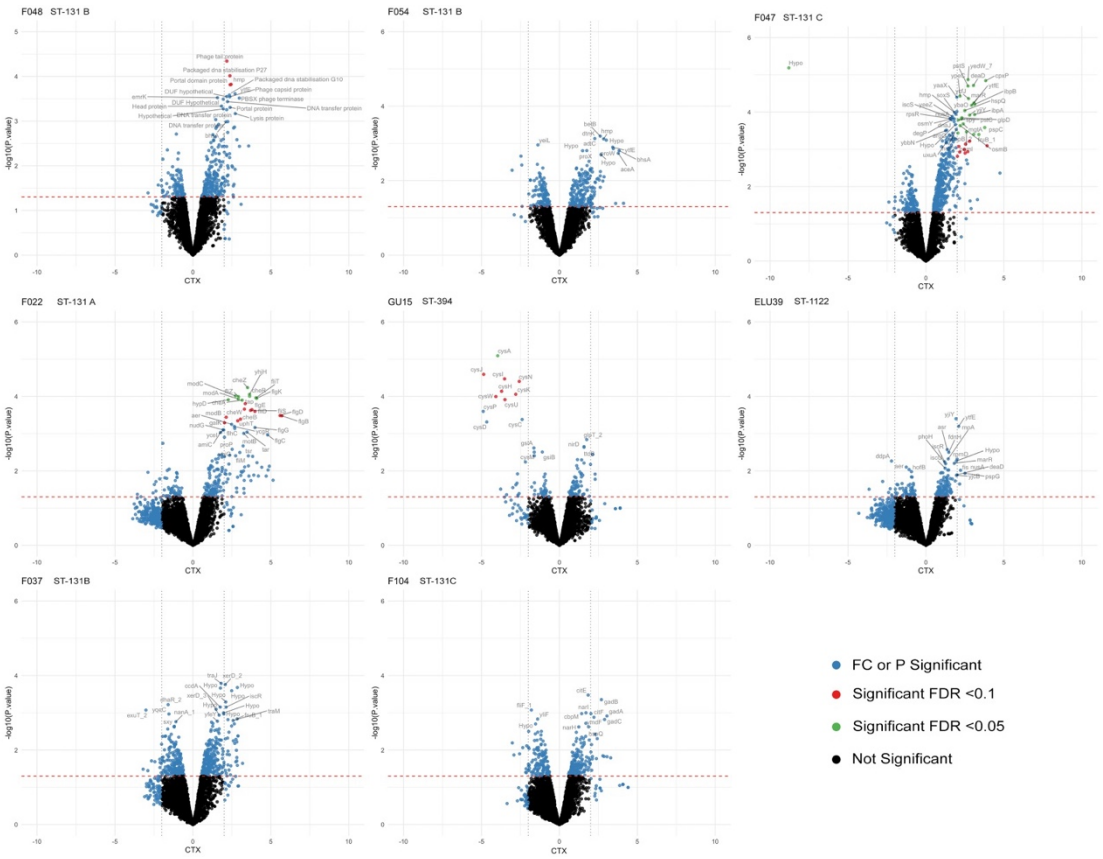
F048 ST-131 B
F054 ST-131 B
F047 ST-131 C
F022 ST-131 A
GU15 ST-394
ELU39 ST-1122
F037 ST-131B
F104 ST-131C
-log10(P.value)
CTX
FC or P Significant
Significant FDR <0.1
Significant FDR <0.05
Not Significant

807

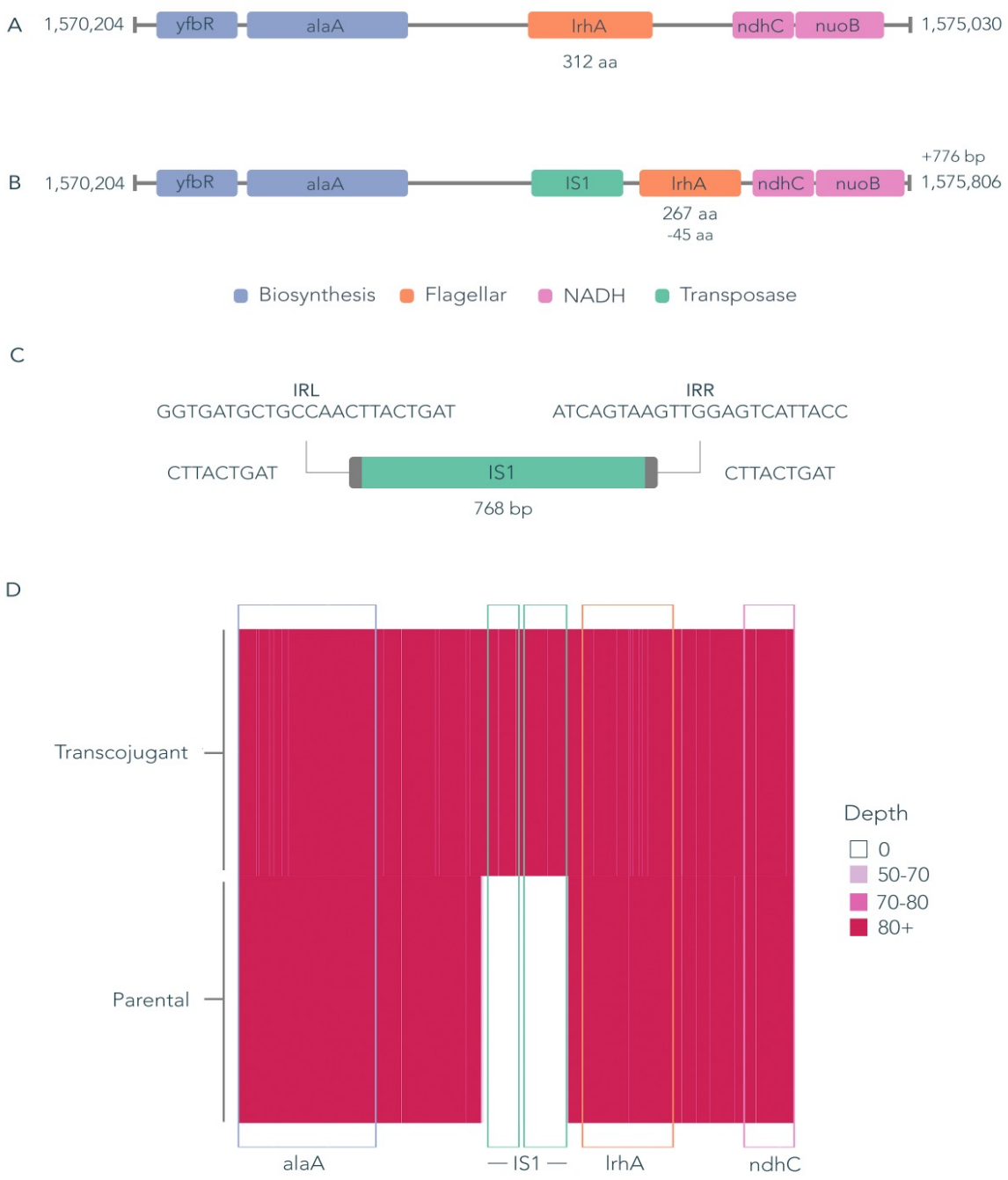
A
1,570,204
yfbR
alaA
lrhA
ndhC
nuoB
1,575,030
312 aa
B
1,570,204
yfbR
alaA
IS1
lrhA
ndhC
nuoB
+776 bp
1,575,806
267 aa
-45 aa
Biosynthesis
Flagellar
NADH
Transposase
C
IRL
GGTGATGCTGCCAACTTACTGAT
IRR
ATCAGTAAGTTGGAGTCATTACC
CTTACTGAT
IS1
CTTACTGAT
768 bp
D
Transcojugant
Parental
Depth
0
50-70
70-80
80+
alaA
IS1
lrhA
ndhC

808

Cellular Processes and Signalling
Information Storage and Processing
Metabolism
Poorly Characterised
Gene Expression (fold change log2)
Up (5)
Down (-5)
Isolate: F048 F054 F047 F022 GU15 EL39 F037 F104
Sequence Type: 131-B 131-B 131C 131-A 394 1122 131-B 131-C
Phylogroup: B2 B2 B2 B2 D A B2 B2
UPGMA Clustering:

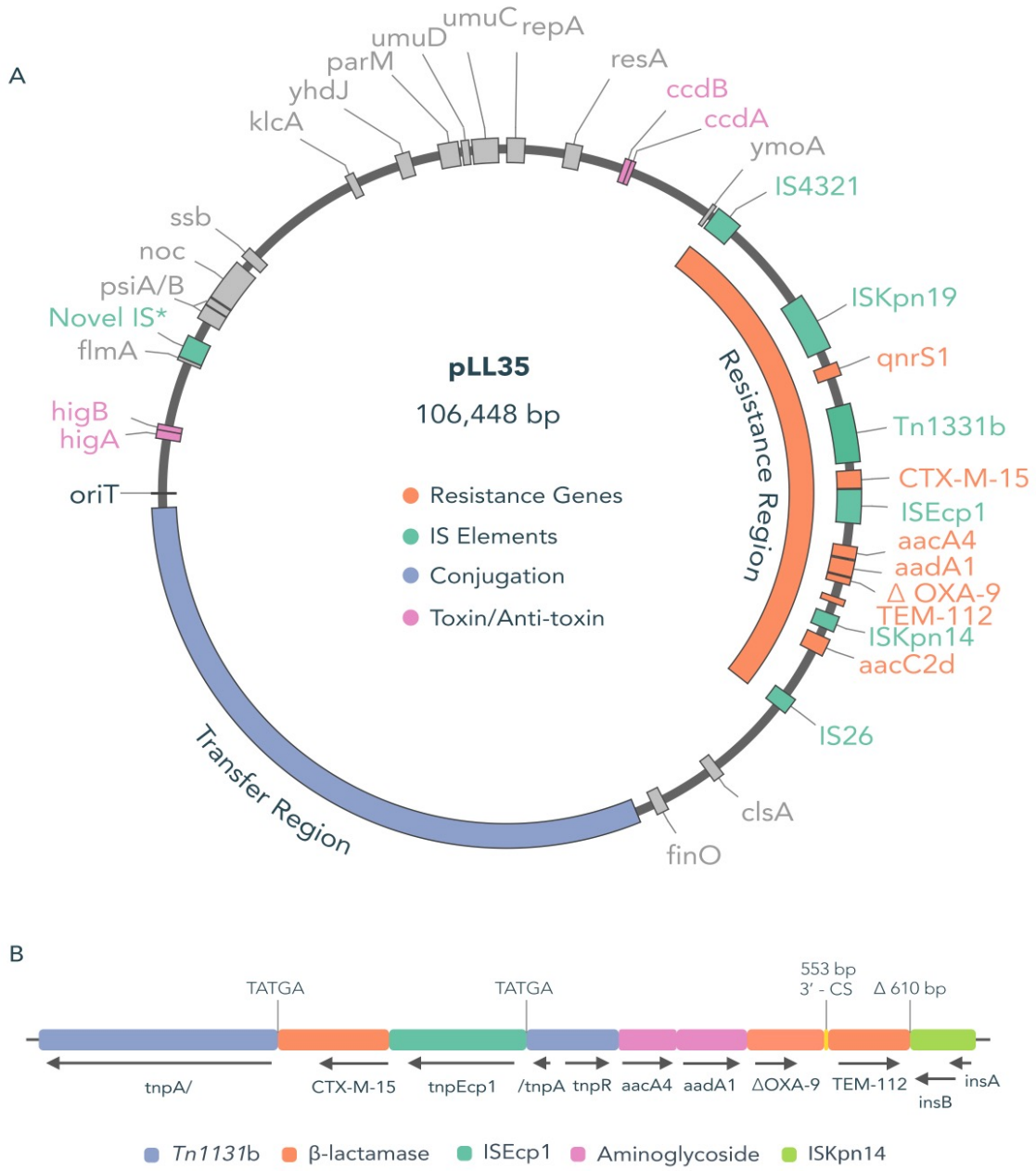
A
umuC
repA
umuD
parM
yhdJ
klcA
resA
ccdB
ccdA
ymoA
IS4321
ssb
noc
psiA/B
Novel IS*
flmA
higB
higA
oriT
ISKpn19
qnrS1
Tn1331b
CTX-M-15
ISEcp1
aacA4
aadA1
Δ OXA-9
TEM-112
ISKpn14
aacC2d
IS26
clsA
finO
pLL35
106,448 bp
Resistance Genes
IS Elements
Conjugation
Toxin/Anti-toxin
Resistance Region
Transfer Region
B
TATGA
TATGA
553 bp
3' - CS
Δ 610 bp
tnpA/
CTX-M-15
tnpEcp1
/tnpA
tnpR
aacA4
aadA1
ΔOXA-9
TEM-112
insA
insB
Tn1131b
β-lactamase
ISEcp1
Aminoglycoside
ISKpn14

810

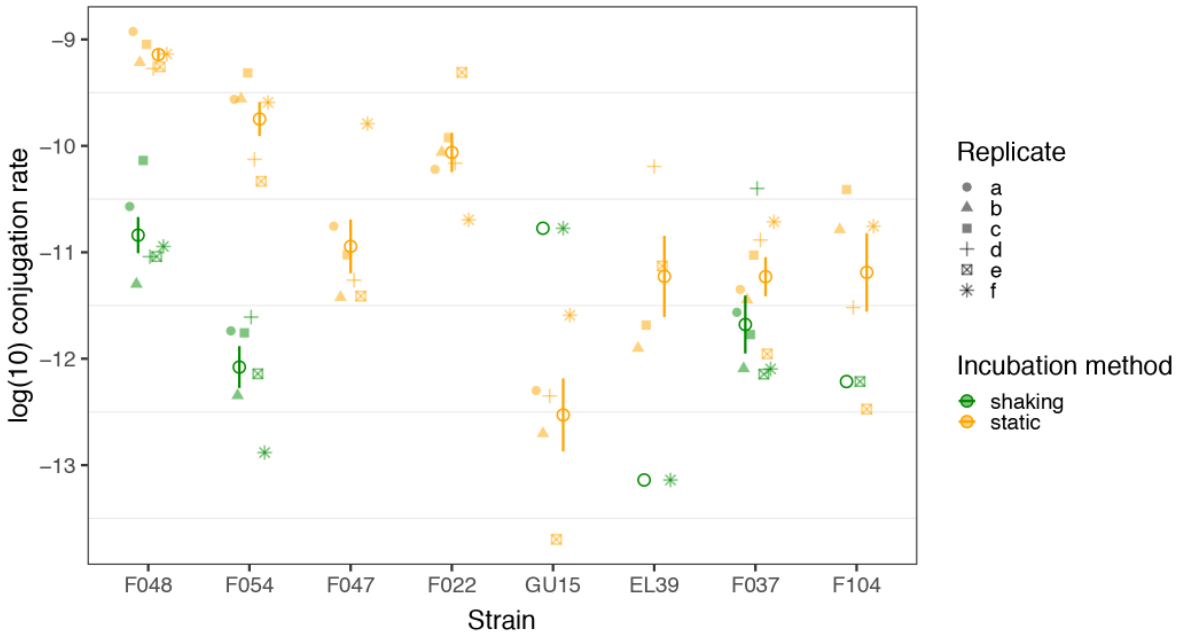
log(10) conjugation rate
−9
−10
−11
−12
−13
F048
F054
F047
F022
GU15
EL39
F037
F104
Strain
Replicate
a
b
c
d
e
f
Incubation method
shaking
static

811

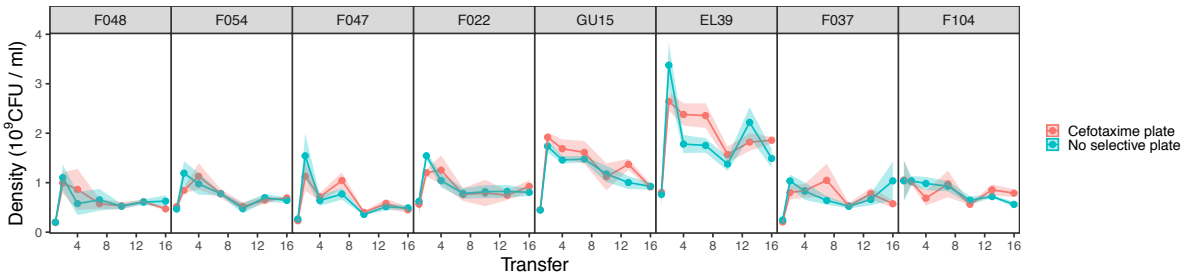
F048
F054
F047
F022
GU15
EL39
F037
F104
Density ($10^8$CFU / ml)
Transfer
Cefotaxime plate
No selective plate

812

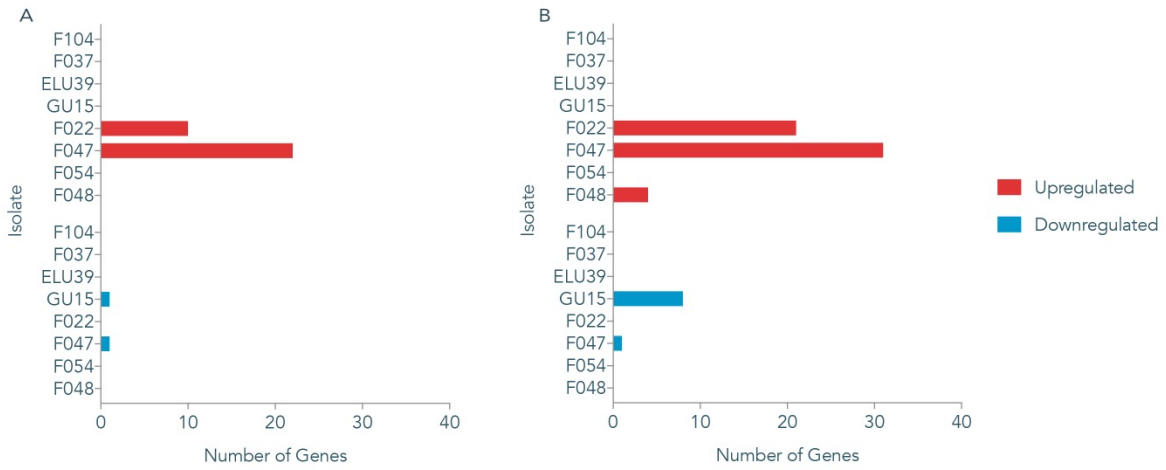
A
B
Isolate
F104
F037
ELU39
GU15
F022
F047
F054
F048
Number of Genes
Upregulated
Downregulated

813

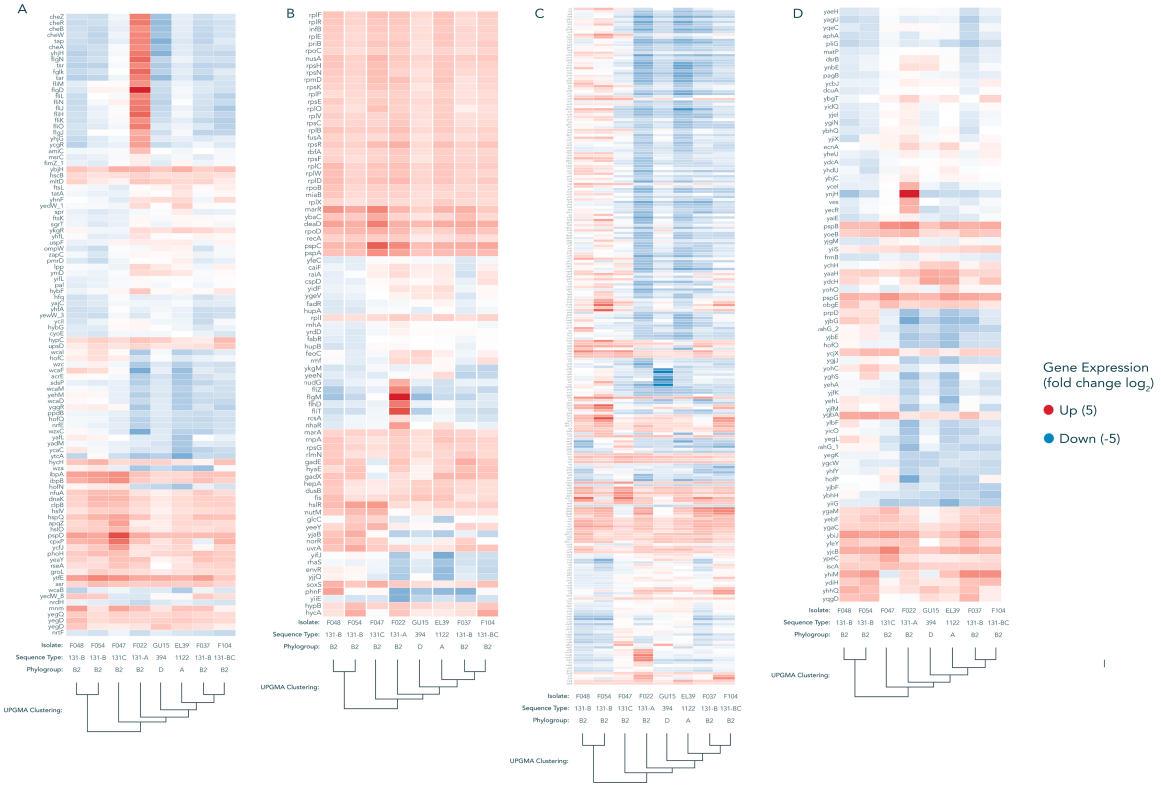
A
B
C
D
Isolate: F048 F054 F047 F022 GU15 EL39 F037 F104
Sequence Type: 131-B 131-B 131C 131-A 394 1122 131-B 131-BC
Phylogroup: B2 B2 B2 B2 D A B2 B2
UPGMA Clustering:
Gene Expression
(fold change log2)
Up (5)
Down (-5)

814

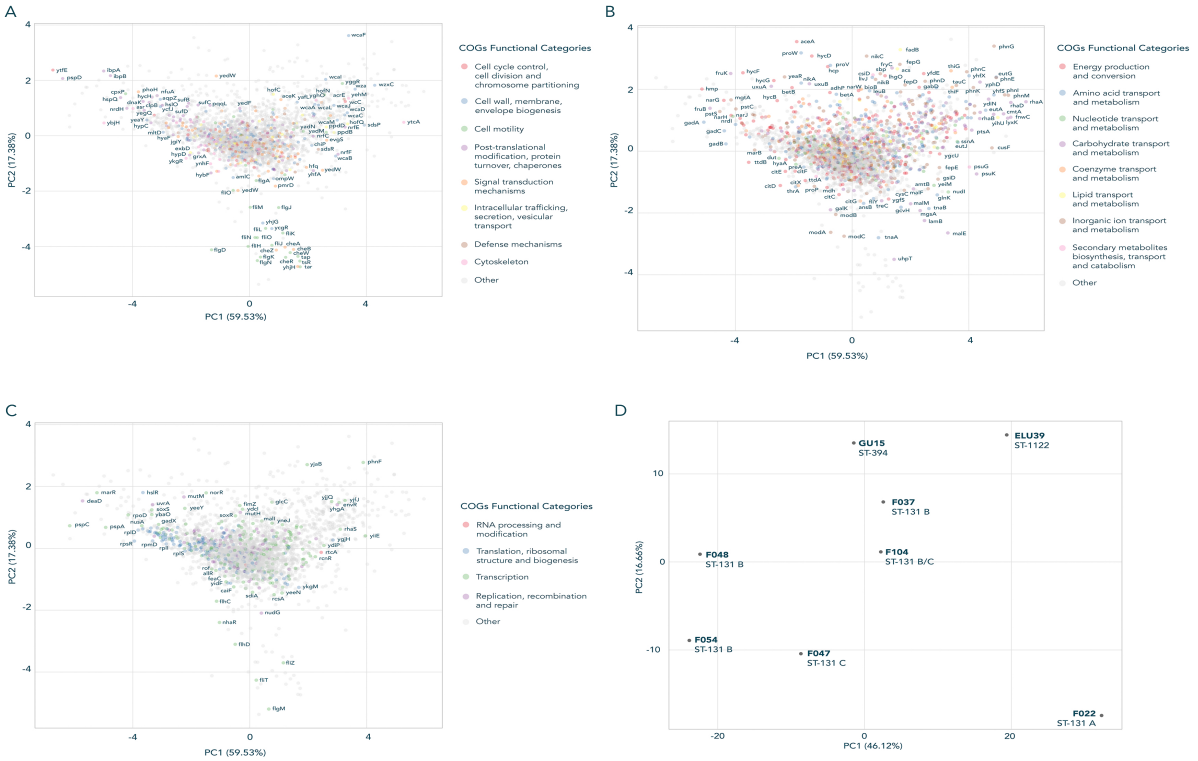
A
B
C
D
PC1 (59.53%)
PC2 (17.38%)
PC2 (17.39%)
PC1 (46.12%)
PC2 (16.66%)
COGs Functional Categories
Cell cycle control, cell division and chromosome partitioning
Cell wall, membrane, envelope biogenesis
Cell motility
Post-translational modification, protein turnover, chaperones
Signal transduction mechanisms
Intracellular trafficking, secretion, vesicular transport
Defense mechanisms
Cytoskeleton
Other
Energy production and conversion
Amino acid transport and metabolism
Nucleotide transport and metabolism
Carbohydrate transport and metabolism
Coenzyme transport and metabolism
Lipid transport and metabolism
Inorganic ion transport and metabolism
Secondary metabolites biosynthesis, transport and catabolism
RNA processing and modification
Translation, ribosomal structure and biogenesis
Transcription
Replication, recombination and repair
GU15 ST-394
ELU39 ST-1122
F037 ST-131 B
F048 ST-131 B
F104 ST-131 B/C
F054 ST-131 B
F047 ST-131 C
F022 ST-131 A

815

816